

Statistics and probability analysis of vehicle overloads on a rigid frame bridge from long-term monitored strains

Yinghua Li, Liqun Tang*, Zejia Liu and Yiping Liu

School of Civil Engineering and Transportation, State Key Laboratory of Subtropical Building Science, South China University of Technology, Guangzhou, China. 510640

(Received December 7, 2011, Revised February 6, 2012, Accepted February 29, 2012)

Abstract. It is well known that overloaded vehicles may cause severe damages to bridges, and how to estimate and evaluate the status of the overloaded vehicles passing through bridges become a challenging problem. Therefore, based on the monitored strain data from a structural health monitoring system (SHM) installed on a bridge, a method is recommended to identify and analyze the probability of overloaded vehicles. Overloaded vehicle loads can cause abnormality in the monitored strains, though the abnormal strains may be small in a concrete continuous rigid frame bridge. Firstly, the abnormal strains are identified from the abundant strains in time sequence by taking the advantage of wavelet transform in abnormal signal identification; secondly, the abnormal strains induced by heavy vehicles are picked up by the comparison between the identified abnormal strains and the strain threshold gotten by finite element analysis of the normal heavy vehicle; finally, according to the determined abnormal strains induced by overloaded vehicles, the statistics of the overloaded vehicles passing through the bridge are summarized and the whole probability of the overloaded vehicles is analyzed. The research shows the feasibility of using the monitored strains from a long-term SHM to identify the information of overloaded vehicles passing through a bridge, which can help the traffic department to master the heavy truck information and do the damage analysis of bridges further.

Keywords: bridges; overloaded vehicles; probability analysis; long-term health monitoring; wavelet transform; FEM

1. Introduction

Overloaded vehicle in many countries (especially in developing countries) is a widespread problem resulting in damage of bridges ahead of time and brings in huge economic losses. Although the stresses induced by overloads are usually below the strength or yield limit of materials used in the bridges, the cyclic stress level are increased, and this may shorten the life of materials and cause unexpected destruction of bridges. How to learn the overloading status and trend of a bridge conveniently becomes very importance.

At present, there are many SHMs already or to be built (Casciati *et al.* 2003, Wang *et al.* 2004, Pines *et al.* 2002, Mufti *et al.* 2002, Wu *et al.* 2003, Chan *et al.* 2006, Kim *et al.* 2007, Frangopol *et al.* 2008), which intended to lean the health of bridges. As for the bridge SHM, data analysis and

*Corresponding author, Professor, E-mail: lqtang@scut.edu.cn

evaluation is the most critical and difficult part. However, there are only several methods (mainly based on vibration) developed for structural damage identification (Achenbach *et al.* 1997, Aktan *et al.* 1996, Alampalli *et al.* 1994). With the development of signal processing technology (Chang *et al.* 1999, Balageas *et al.* 2002), real-time analysis and processing of measured data collected from bridge monitoring systems becomes possible. Based on the wavelet transform method, Moyo and Brownjohn (2002) decomposed the strain data collected from a bridge monitoring system by means of wavelet, a statistical analysis was used to process the wavelet coefficient of time series for detecting outliers, and better identification effects had been obtained. Omenzetter, etc. (2004) made use of the multivariate statistical method and the vector autoregressive moving average model to study the association among multi-channel strain wavelet transform data and the identification of the outliers of the monitored data, and it indicated that the abnormal values had strong localized features with the sensors affected significantly only in one concrete placing segment. However, the identification of overloaded vehicles based on bridge monitoring data has not been reported so far. In this paper, we focus on this problem.

2. The long-term SHM installed on the background bridge

2.1 Architecture of SHM

The background bridge is called Zhaoqing West River Bridge (Fig. 1), which locates in Zhaoqing City, Guangdong Province, China. The first span is 145.4 m long, the sixth span is 87 m long, and the 4 central spans are all 144 m long (Fig. 1). The cross section of box girder is shown in Fig. 2. The heights, thickness of base plate and web plate vary from 8 m to 2.8 m, 1 m to 0.32 m and 0.9 m to 0.45 m respectively in cross sections from the supporting base to the mid-span.

The cross sections in the box girder of the bridge with the sensors locates near piers, mid-spans and 1/4 spans, and there are total 20 sections shown in Fig. 1 with given names. The embedded locations of strain sensors in each section are illustrated in Fig. 2 with given numbers.

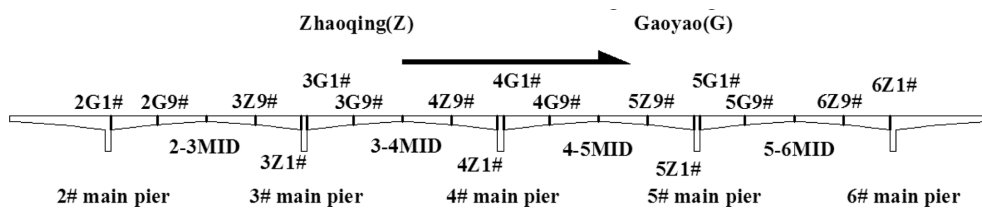


Fig. 1 Section locations of sensors embedded in the SHM in the Bridge

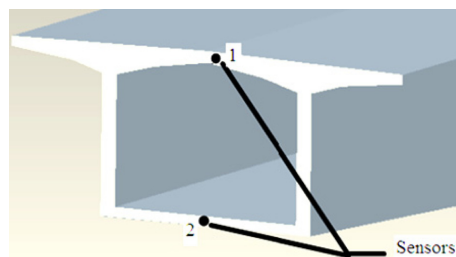


Fig. 2 Positions of the embedded sensors in bridge cross section



Fig. 3 A vibrating wire strain gauge installed inside the bridge before the concrete casted

Table 1 Basic parameters of JMZX-215 type strain gauge

Name	Range	Sensitivity	Gauge length	Remarks
Intelligent digital vibrating wire strain gauge	0~3000 $\mu\epsilon$	1 $\mu\epsilon$	157 mm	Strain gauge embedded in concrete

Sensors were installed inside of concrete during the construction of the bridge, and each sensor is apart from concrete surface at least 10 cm. The type of the sensor is a vibrating wire strain gage called JMZX-215, in which a temperature sensor included (Shown in Fig. 3). Table 1 shows the basic measurement parameters of the sensor. The sampling period of each sensor is 1 hour.

2.2 Basic features of monitored strains with time

The bridge has been monitored more than 4 years so far. Here, the data collected from the sensors named 2-3MID-2, 5-6 MID-2, 4Z9h-1 and 3G1h-1 (The chosen monitoring time range: from January 2009 to January 2010) is selected as example. Sensors 4Z9h-1 and 3G1h-1 locate on the top plate of the bridge, while 2-3MD-2 and 5-6MID-2 locate on the bottom plate of the bridge.

In fact, there are tens of thousands of data collected from the SHM. From Fig. 4, it can be found that the strains of four sensors have stable traces with time and the signal of the two sensors in base plates basically has no interference, but the two sensors in top plates existed many singular strains which’s variations are even greater than theirs ordinary values. The singular strains may be some strong disturbances induced by thunder like natural electric jamming. Some gaps appear in the data

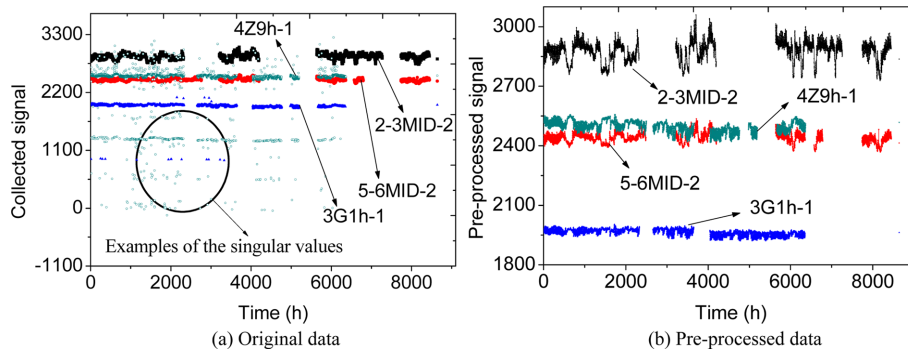


Fig. 4 Original and pre-processed data collected from the SHM

shown in Fig. 4, because some data was not collected due to data acquisition system fault. So, the monitored data should be pre-processed firstly to erase the singular values and the data will be imported segment by segment for processing to skip the gaps. The principle of deleting the singular values is as follows: 1) find out the difference between the values of each sampling point and its previous sampling point; 2) if the value of the difference is great than 200 micro-strain (engineering experience value (Zhang *et al.* 2007)), the signal of this sampling point is regarded as singular value; 3) the identified singular value will be removed and replaced with a value of its adjacent sampling points which will retain normality in the signal.

3. Application of wavelet analysis to SHM

3.1 Strain features in bridges

For each sensor, the recorded strains $\varepsilon_1, \varepsilon_2, \dots, \varepsilon_n$, can be organized as a time series $\varepsilon(t_i)$. Actually, the measured strain consists of three parts

$$\varepsilon(t_i) = \varepsilon_{C,t_i} + \varepsilon_{T,t_i} + \varepsilon_{R,t_i} \quad (1)$$

where ε_{C,t_i} represents the time-dependent strain due to concrete creep and shrinkage; ε_{T,t_i} represents the strain induced by thermal dilation of concrete; ε_{R,t_i} represents the strain due to random loads including vehicle loads, ground motions, accidents and so on.

Typical curves used to describe the section ε_{C,t_i} are shown in Fig. 5. From Fig. 5, the variation of the creep strain within one year is not sensitive to short time scale. $\varepsilon_{T,t}$ is induced by daily and seasonal variations in temperature, while the change cycle of daily temperature variation is 24 h and the change cycle of seasonal temperature variation is much longer.

The measured strains couple three components, and the strain components ε_{C,t_i} and ε_{T,t_i} vary gradually compared with sampling time scale (1 hour), which will not induce the sudden change feature in the profile of the time series $\varepsilon(t_i)$. Mays and Tilly (1982) proposed that the loading frequency of the traffic on highway bridges could be equivalent to 1Hz, which means that the vehicle loads (There are other unusual events, such as heavy rainfall, etc.) may let the component ε_{R,t_i} vary obviously when vehicles pass through bridges, and the values will illustrate abnormal

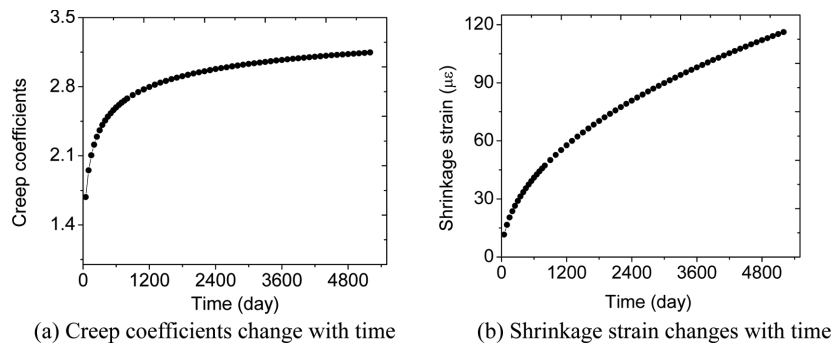


Fig. 5 Typical curve of creep and shrinkage strain against time of concrete

features compared with strains sampled at neighboring times. The larger vehicle load induces more remarkable abnormal feature. This property in the monitored strains $\varepsilon(t_i)$ will be used to identify the overloaded vehicles.

3.2 Wavelet analysis in time series of monitored strains

There are many monitored data in each time series $\varepsilon(t_i)$. So, it has some difficulties to determine the abnormal points in the abundant monitored data. Here, the wavelet analysis is introduced to help to determine the abnormal points in the time series $\varepsilon(t_i)$, for which the wavelet analysis can decompose the data in different time scales and the strain analysis shows that three kinds of strain in Eq. (1) do have different time scales.

Given a function $Y(t) \in L^2(R)$, the discrete wavelet transform of $Y(t)$ consists of wavelet coefficients and scaling coefficients, given by

$$\begin{cases} d_{j,k} = \int_{-\infty}^{\infty} Y(t) \psi_{j,k}^*(t) dt, (j = 1, 2, \dots, J,) \\ c_{J,K} = \int_{-\infty}^{\infty} Y(t) \phi_{J,K}^*(t) dt, (j = 1, 2, \dots, J,) \end{cases} \quad (2)$$

$\psi_{j,k}(t) = 2^{-j/2} \psi(2^{-j}t - k)$, $\phi_{j,k}(t) = 2^{-j/2} \phi(2^{-j}t - k)$, where “*” denotes the complex conjugate, $J = \log_2(n)$ and n is the number of samples. $Y(t)$ can be reconstructed from the coefficients by

$$\begin{cases} Y(t) = S_J + \sum_{j=1}^J D_{j,k} \\ S_J = c_{J,K} \phi_{J,K}(t) \end{cases} \quad (3)$$

where S_J is an approximation of $Y(t)$ at level $j = J$, and $D_{j,k}$ represents the difference between two successive approximations.

By means of Daubechies family wavelet analysis of strain data in multiple scales, Moyo and Brownjohn (2002) pointed out that ε_{R,t_i} could be isolated from the strain $\varepsilon(t_i)$ by decomposing strain data into 2 scales and suggested the wavelet strain model as follows

$$\varepsilon(t) \approx c_{J_c^l} \phi_{J_c^l}^l(t) + \left[A + \sum_{j=J_c^l}^{J_c^l} d_{J_c^l} \psi_{J_c^l}^l(t) \right] + \sum_{j=J-3}^{J-4} d_{jk} \psi_{jk}(t) + \sum_{j=J}^{J-1} d_{jk} \psi_{jk}(t) \quad (4)$$

$$\varepsilon_{T,t} \equiv \left[A + \sum_{j=J_c^l}^{J_c^l} d_{J_c^l} \psi_{J_c^l}^l(t) \right] + \sum_{j=J-3}^{J-4} d_{jk} \psi_{jk}(t), \quad \varepsilon_{C,t} \equiv c_{J_c^l} \phi_{J_c^l}^l(t) \quad \text{and} \quad \varepsilon_{R,t} \equiv \sum_{j=J}^{J-1} d_{jk} \psi_{jk}(t)$$

where $c_{J_c^l}$ is scaling coefficient associated with creep due to sustained loading and $d_{J_c^l}$ is wavelet coefficient associated with strains due to temperature variations. It is proposed that wavelet coefficients d_{Jk} and $d_{(J-1)k}$ (or detail coefficients D_{Jk} and $D_{(J-1)k}$) are associated with changes occurring in the random component of $Y(t)$, i.e., ε_{R,t_i} in Eq. (1).

3.3 Detection of anomalous structural behavior

If wavelet coefficients \bar{d}_{jk} is considered with random changes in $Y(t)$, these coefficients consist of changes in average of $Y(t)$ and noise associated with random sampling, given by

$$\bar{d}_{jk} = d_{jk} + \xi_{jk} \quad (5)$$

where ξ_{jk} is white-noise with zero mean and variance σ^2 .

In this paper, the aim is to identify wavelet coefficients that represent random changes at low scales s_j . With normal conditions, strain $Y(t)$ vary smoothly with time, but an abrupt change would cause discontinuity in the variation of $Y(t)$. Then, the corresponding \bar{d}_{jk} is significantly higher than others in its neighborhood (Daubechies (1997)). Hence, sudden changes in strain data can be detected by means of checking the magnitudes of wavelet coefficients against a threshold. Donoho and Johnstone (Donoho *et al.* 1994) suggested the threshold coefficient as a modified version of universal noise threshold, given by (Abramovich *et al.* 2000)

$$\lambda = \sigma(\sqrt{4(\log n + \log \log n)}) \quad (6)$$

The noise level in the monitored data is generally unknown and should be estimated from the monitored data. In this paper, the method suggested by Donoho and Johnstone (Donoho *et al.* 1995) is adopted, which uses wavelet coefficients at the highest level of resolution to estimate σ , given by

$$\sigma = \frac{\text{median}(|d_{J-1,k} - \text{median}(d_{J-1,k})|)}{0.6745} \quad (7)$$

where $J = \log_2(n)$.

Then, by means of recording the recognized locations of the detail coefficients which are greater than the threshold, the potential abnormal signals may be extracted in the strain time series. For each picked up signal previously, it is needed to compare its value with its “normal” value. Cubic Spline interpolation is applied here to determine the “normal” values of the corresponding abnormal signals.

As for the identification of overloaded vehicles, the differences between the abnormal signal and the fitted “normal” values will be compared with the strain threshold (Simulated by FEM in the following article and denoted by ε_{qc}), which is used for the identification of overloaded vehicles.

4. Abnormal events analysis and determination of strain threshold

4.1 Calibration of the reliability of FEM model and SHM measurement

The extracted strains via wavelet analysis may be induced by heavy vehicles. Now the key is how to identify the abnormal strains induced by overloaded vehicles. Therefore, FEM technology is used to learn the strain value generated in the sensor's location when overloaded vehicles are passing through the bridge, and determine the strain threshold induced by overloaded vehicles. Here, the sub-model technology will be used to learn the local responses in the bridge (ANSYS company 1999, Xie *et al.* 2000), which helps to simplify the analysis model and get enough analysis accuracy.

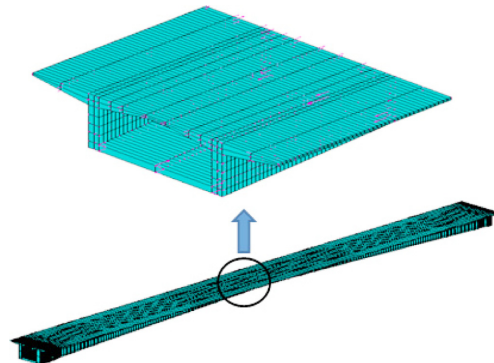


Fig. 6 Schematic and mesh mode of FEM sub-model

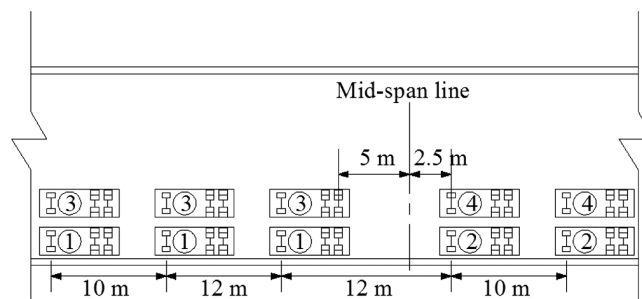


Fig. 7 Loading Scheme of the loading capacity test

A FEM sub-model of Zhaoqing West River Bridge is set up including the girder between the main pier 2# and the main pier 3# (Shown in Fig. 6). In this model, a 3D element with the shortest length 0.25 m is used to simulate concrete, and there are 37,388 elements and 57600 nodes in the sub-mode.

In order to check the reliability of both the finite element model and the measurement results of SHM, a calibration work has been done on a loading capacity test of the bridge before the bridge came into service. On the test, utmost ten QC-20 main vehicles (a truck loading model with the weight 300 kN defined in a Chinese Specification JTG D60-04 (2004)) were used, and they were divided into four loading levels: 900 kN, 1500 kN, 2400 kN, 3000 kN. Fig. 7 shows the loading

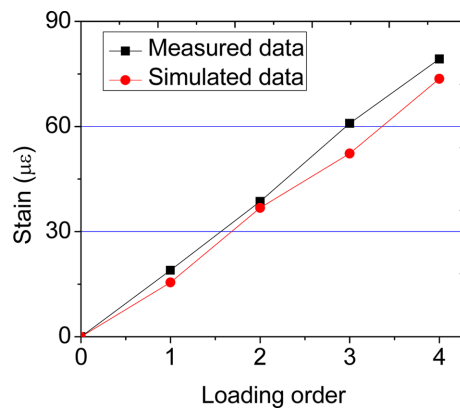


Fig. 8 Comparison between the simulated data and the monitored data (Corresponding to the sensor 2-3MID-2)

distribution of each loading level, where first loading level included trucks with “①” and second loading level included trucks with “①” and “②”, and so on. Fig. 8 illustrates the comparison between the measured results and FEM results at the position sensor 2-3MID-2 located, and the two results have a good agreement, which means that both results of the two methods are reliable.

4.2 Determination of the strain threshold

In this paper, the key is to design a reasonable load in FEM model to represent the overloaded vehicle. Here we introduce three kinds of vehicle loads to help determining the threshold:

- (1) A QC-20 heavy truck with about double standard load. The axle load distribution is shown in Fig. 9, and such load will “move” along the span with speed 15 m/s to learn the response strength of the sensor at the mid-span.
- (2) Two QC-20 main trucks side by side and each truck with standard load (The axle load distribution is similar to Fig. 9), and the load also “moves” along the span with speed 15 m/s;
- (3) A distributed loads by a group of vehicles with standard loads according to a Chinese Specification JTG D60-04 (2004), the loading distribution can be seen in Fig. 10.

In this article, we do not consider an extreme situation e.g., one lane or two lanes fully loaded by QC-20 vehicles, its effect on the monitored data can be ignored (Nowak 1993).

Strain values generated under vehicles passing through the girder in the above case (1) and (2), at the sensor 2-3MID-2, are shown in Fig. 11, the maximum strain is about $18 \mu\epsilon$. In case (3), the strain value is about $17 \mu\epsilon$ in the same position.

Vehicle loads also have impact effect on bridges. Hwang and Nowak (Hwang *et al.* 1991) suggested that the dynamic deflection is a function of three major parameters: road surface roughness, bridge dynamics (frequency of vibration) and vehicle dynamics (suspension system), and which do not depend on truck weight. According to a Chinese Specification JTG D60-04, the impact coefficient of vehicle load takes the value 0.081.

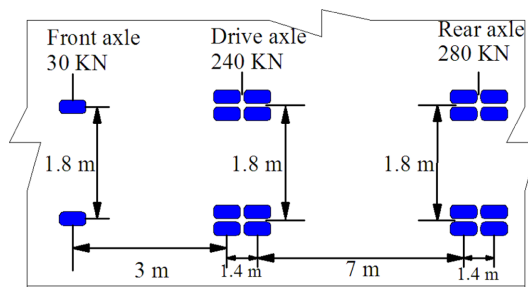


Fig. 9 Load’s distribution of QC-20 overloaded vehicle

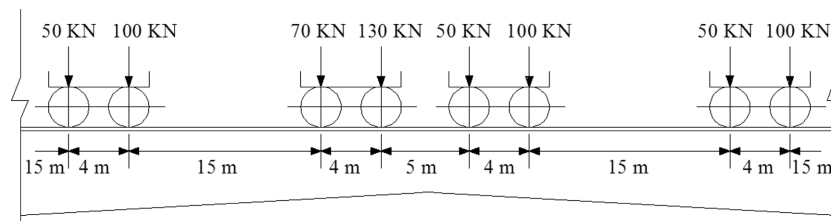


Fig. 10 Loading positions and manners of a group of normal vehicles

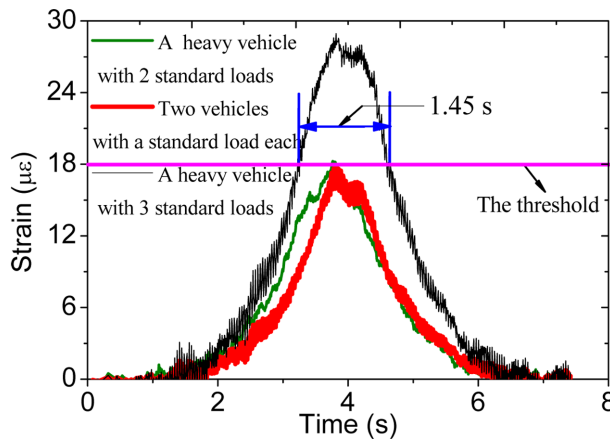


Fig. 11 Strain responses in the mid-span base plate center

By considering the three vehicle loading effects and the dynamic properties, we recommended that the threshold ε_{qc} takes the value $18 \mu\varepsilon$, which may be too conservative to determine the overloaded vehicle number. Anyhow, in the view of damage of bridges, the lower overload induces smaller damage to bridge. So, such definition is acceptable.

4.3 Captured probability of an overloaded vehicle passing the bridge by the SHM

The time of a vehicle passing through a bridge is less than 48s with the standard speed 15 m/s, which means that an overloaded vehicle can be captured utmost one time by the SHM with sampling period 1 hour. The time of a vehicle passing through a main span is approximately 8 seconds, but the time of a vehicle captured as an overloaded vehicle is far less than 8 second with the strain threshold $18 \mu\varepsilon$ (Fig. 11). Therefore the captured probability of an overloaded vehicle is very low. The more overload is the larger captured probability. For an example, if a vehicle with 3 times of a QC-20 standard load (very common in mainland China) (Fig. 11), the time interval with strain over the threshold is 1.45s, its captured probability is about 0.0403% ($1.45/3600$).

4.4 Other potential effects of abnormal events

Another unusual event that bridges often encounter is torrential rain, which may affect the determination of the overload. The raindrop impact force can be converted to uniform load on the finite elements and is given by the following formula (Ren 2007)

$$\begin{cases} F_d = \frac{2}{9} \rho \pi d^3 n V_s^2 b \\ n(d) = n_0 \exp(-\Lambda d) \end{cases} \quad (8)$$

where ρ is the density of water, d is the diameter of raindrop and takes 2.76 mm, n is the distribution function of the raindrop diameter, V_s is the falling speed of raindrop and takes 7.7 m/s, b is the section width of the bearing force components and takes 12.5 m, $n_0 = 8 \times 10^3$ (drip)/ m^3/mm , Λ is the slope factor and $\Lambda = 4.1I^{0.21}$ (I is the rainfall intensity and takes 200 mm/h). With the heavy rain load calculated by

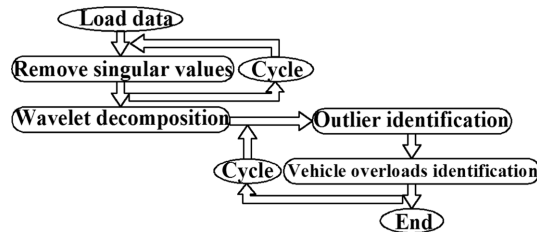


Fig. 12 Flow chart of identification

formula (8) in the sub-model analysis, the strain value at the location of sensor 2-3MID-2 induced by the rainstorm is about $2\sim 3 \mu\epsilon$, which is quite small than that induced by the QC-20 vehicles.

Historically, seismic activity level is very low in the region. Therefore, in this work we do not study the impact of the ground motion on the background bridge.

As for the continuous rigid frame concrete bridge, experience teaches that wind may have a great importance with regard to the balanced cantilever erection stages (Schmidt *et al.* 2003). After construction, the wind load effect can be neglected.

From the above analysis, we may conclude if the abrupt increment of strain is larger than the threshold ϵ_{qc} , the increment can be regarded as a strain induced by heavy vehicle.

5. Identification of overloaded vehicles

5.1 Method of identification

From the view above, we suggest a method to identify the strains generated by overloaded vehicles from the monitored data (Fig. 12):

- (1) Selection suitable initial data. As there are many sensors in the SHM, it is important to select data collected from the sensors that are sensitive to vehicle loads. As for the system mentioned in this article, it is obvious to select the sensors located in the mid-span base plate;
- (2) Pre-processing the initial data. By means of comparing the initial data with the limit strain of concrete, the singular data will be filtered from the initial data and replaced with a value of its adjacent sampling points. Some gaps appear in the data shown in Fig. 4, and therefore the data will be imported segment by segment for processing to skip the gaps;
- (3) Abnormal events identification. Decompose the pre-processed data by the use of wavelet analysis and calculate the wavelet coefficient thresholds; compare the wavelet coefficients with their own thresholds for each selected sensor to pick up the potential data induced by the overloaded vehicles;
- (4) Heavy vehicle identification. Find the differences between the potential data and the Cubic Spline fitted values of their neighborhoods, and compare the differences with the strain threshold ϵ_{qc} to identify the overloaded vehicles;
- (5) Statistical analysis of the identified data. Due to the random environment suffered by bridges, it is necessary to do statistical analysis of the identified data.

As for the proposed methodology above, the wavelet analysis provide a fast arithmetic to determine the abnormal data (potential overload signal) from abundant monitored data; then, for each abnormal data,

we need to calculate its strain change amplitude and compare it with the threshold to judge whether the signal is a overload signal or not.

5.2 Example of heavy vehicle identification process

Sensors embedded in the mid-span cross sections are more sensitive on the random events, especially in the mid-span base plate. In the following, the monitored data collected from the sensors 2-3MID-2 and 5-6MID-2 embedded in the mid-span base plate (The signal collected from the sensors embed in the base plate is stable and has no interference) will be selected for the analysis of the heavy vehicle identification.

The recognition process suggested previously is achieved by developed computer program. In order to show the features in the identification process, 1 month data (January 2010) collected from the sensor 2-3MID-2 is firstly selected as an example, shown in Fig. 13:

Db (4) wavelet is applied to decompose the measured data in Fig. 13 into 2 layers, and the abrupt changes in strain data are detected by checking the magnitude of the wavelet coefficients against the threshold λ . Then, the abnormal strains in the time series can be located (Fig. 14).

Finally, based on step (4) in the previous section, overloaded vehicles and the results obtained are shown in Fig. 15. Seen in Fig. 15, the jump direction of the identified points is all the same. Hence, the identified data is reliable.

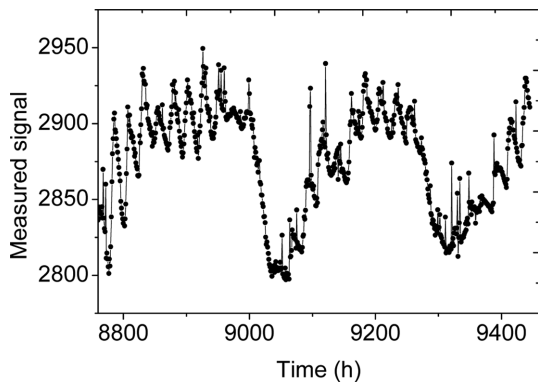


Fig. 13 Filtered data of sensor 2-3MID-2 in Jan. 2010

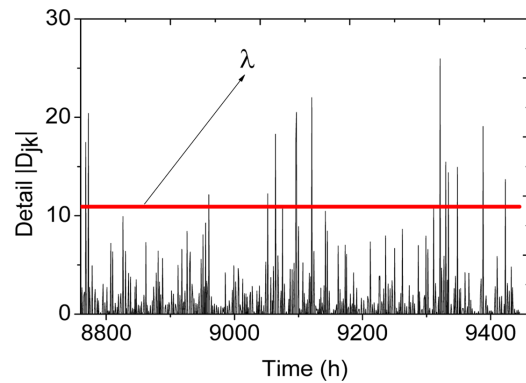
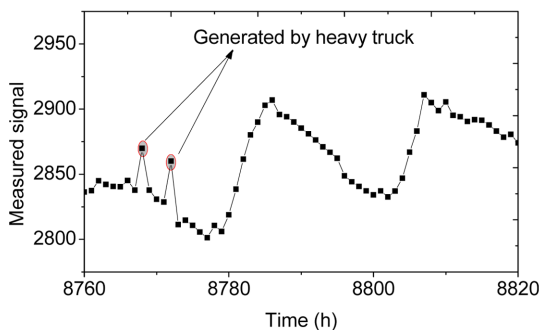
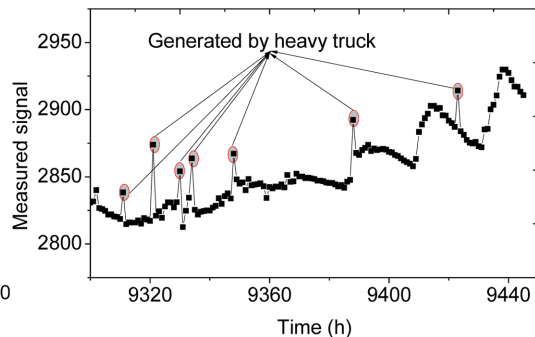


Fig. 14 Detail of wavelet coefficients of example data



(a) Sensor 2-3MID-2



(b) Sensor 2-3MID-2

Fig. 15 Identified results of the heavy vehicles

5.3 Verification of the rationality of the noise threshold in wavelet analysis

In the identification processing suggested above, there are two key steps: the first step, the comparison of the wavelet coefficients with λ helps us to select the potential data from abundant initial data; the second step, the abrupt increment strains are compared with the threshold ε_{qc} . However, if λ is too large, the identified amount of heavy vehicle may be less; if λ is too small, there may be much calculation in the second step. The overloaded vehicle numbers identified from these two steps by the use of one year data shown in Fig. 4 are listed in Table 2, which indicates: (1) the definition of λ is suitable; (2) the overloaded vehicle numbers accounted from the two sensors in different cross sections are credible.

5.4 Estimation of the overloaded vehicle number

Based on the results from Table 2, there are at least 19 heavy vehicles. As we have already analyzed that the probability of heavy truck is about 0.0403%, we can estimate that overloaded vehicles in 2010 passing through the bridge is about $N=19/(0.0403\%)=47146$, and there is nearly 130 overloaded trucks each day, which is a large number but meeting the reality in China.

5.5 Statistics analysis of heavy vehicles

If an overloaded vehicle was detected through a span of the bridge, it wouldn't be detected through other spans because the sampling time interval is an hour for each sensor. Here, we try to learn rationality of the detected results by comparing the consistency of the statistical properties of overloaded vehicles from sensors in different spans. The statistical information of overloaded vehicles is analyzed from one year data (Seen in Fig. 4) collected from the two sensors 2-3MID-2 and 5-6MID-2. Based on the previously identified number of abnormal signal, the statistical features of the strain data generated by Heavy vehicle are obtained and shown in Fig. 16. Cooper (1996) derived the statistical parameters for live load statistical model from studies of heavily loaded highway sites in the United Kingdom and assumed that the maximum annual live load follows an extreme type I distribution. According to the statistical features shown in Fig. 16, the extreme type I distribution is introduced to depict the distribution

$$p(x) = \alpha \exp(-\alpha(\alpha - \mu) - \exp(-\alpha(\alpha - \mu))) \quad (9)$$

where α is the scale parameter, μ is the location parameter. The parameter values are fitted by the use of least squares method and shown in Table 3.

Seen from Fig. 16, it can be concluded that the main profiles of the statistical features obtained from the two sensors are similar. However, there are some differences. It can be seen that the strain change range identified from sensor 5-6MID-2 is about 18~40 $\mu\varepsilon$ and the identified number of heavy vehicle is somewhat small. Yet, sensor 2-3MID-2 is more sensitive to the abnormal events with the strain change range about 18~60 $\mu\varepsilon$, for which the main reason may be that the actual

Table 2 Identified number of abnormal signal

Sensor ID	By λ	By ε_{qc}
2-3MID-2	74	40
5-6MID-2	103	19

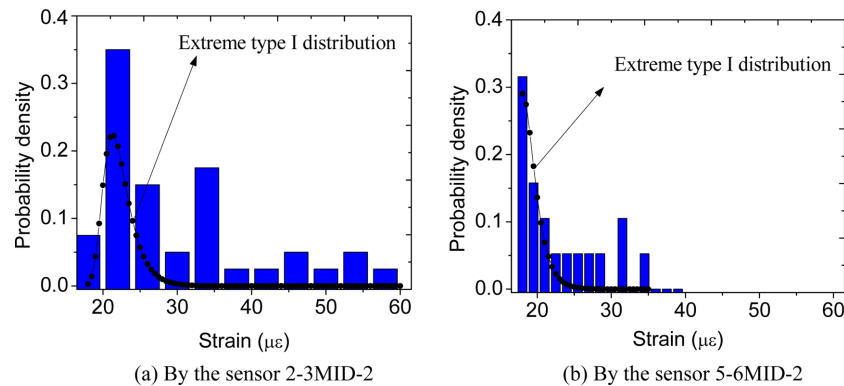


Fig. 16 Statistical results of the identified strain data

Table 3 Fitted parameter values

Parameter	α	μ
By 2-3MID-2	0.6093	23.1509
By 5-6MID-2	0.7894	18.0475

reserve pressure at the location of sensor 2-3MID-2 is much lower than at the location of sensor 5-6MID-2. Also, another reason may be that the amount of the statistical data is a little small. Strain generated by overweight vehicles can achieve more than six times the normal load. Seen in Fig. 16, the strain characteristics of the identified data are in line with the feature of the strain produced by overweight vehicles. Therefore, we believe our identified data is reliable.

6. Conclusions

In this paper, a method is developed for the identification of the overloaded vehicles in the monitored data from long-term SHM. The research shows that the new method introduced here is feasible, which can help the traffic department to master the overloaded vehicle information and do the damage analysis of bridges further. This study also extends the application field of SHM. The method can not fully detect the overloaded vehicles because of the sampling interval of the sensors. Therefore, we estimated a detected probability of a heavy vehicle with normal speed passing the bridge, which helps us to estimate the total overloaded vehicles. Though the estimated result is not very accurate, but it can help to learn the development trend of both heavy vehicle amount and weight. By identifying unusual events (Overloaded vehicle etc.), we can transfer the long-span bridges with SHM to smart structures.

Acknowledgements

The authors wish to express their gratitude to the supports provided by Guangdong Province Natural Science Foundation (05006591) and their partners for their enthusiastic help.

References

- Aktan, A.E., Helmicki, A.J. and Hunt, V.J. (1996), "Issues related to intelligent bridge monitoring", *Proceedings of Building an International Community of Structural Engineers Congress*, Chicago, USA.
- ANSYS company (1999), *Modeling and Meshing Guide*.
- Abramovich, F. and Samarov, A. (2000), *On one-sided estimation of a sharp cusp using wavelets*, department of statistics and operations research, Tel Aviv University, Technical Report RP-SOR-00-02.
- Achenbach, J.D., Moran, B. and Zulfiqar, A. (1997), "Techniques and instrumentation for structural diagnostics", *Proceedings of the International Workshop on Structural Health Monitoring*, Stanford, CA, USA.
- Alampalli, S. and Fu, G. (1994), "Instrumentation for remote and continuous monitoring of structure conditions", *Transport. Res.*, **1432**, 59-67.
- Balageas, D.L. (2002), *Structural Health Monitoring 2002*, Destech Publications, Lancaster.
- Cooper, D.I. Flint and Neill Partnership (1996), "Interim short span bridge assessment loading", *Proceedings of the International Symposium on The Safety of Bridges*, London, UK, July.
- Casciati, F. (2003), *An overview of structural health monitoring expertise within the European Union*, (Eds. Wu, Z.S. and Abe, M.), Structural health monitoring and intelligent infrastructure. Lisse: Balkema; 31-7.
- Chang, F.K. (1999), *Structural Health Monitoring 2000*, Technomic, Lancaster.
- Chan, T.H.T., Yu, L., Tam, H.Y., Ni, Y.Q., Liu, S.Y., Chungb, W.H. and Cheng, L.K. (2006), "Fiber Bragg grating sensors for structural health monitoring of Tsing Ma bridge: Background and experimental observation", *Eng. Struct.*, **28**(5), 648-659.
- Donoho, D.L. and Johnstone, J.M. (1994), *Ideal spatial adaption by wavelet shrinkage*, *Biometrica*, **81**, 425-455.
- Donoho, D.L. and Johnstone, J.M. (1995), "Adapting to unknown smoothness via wavelet shrinkage", *J. Am. Stats. Assoc.*, **90**(432), 1200-1124.
- Daubechies, I. (1992), *Ten lectures on wavelets*, Philadelphia: Society for Industrial and Applied Mathematics.
- Frangopol, D.M., Strauss, A. and Kim, S.Y. (2008), "Bridge reliability assessment based on monitoring", *J. Bridge Eng.*, **13**(3), 258-270.
- Hwang, E.S. and Nowak, A.S. (1991), "Simulation of dynamic load for bridges", *J. Struct. Eng.- ASCE*, **117**(5), 1413-1434.
- Kim, S., Pakzad, S., Culler, D., Demmel, J., Fennes, G., Glaser, S. and Turon, M. (2007), "Health monitoring of civil infrastructures using wireless sensor networks", *Proceedings of the 6th International Symposium on Information Processing in Sensor Networks*, Cambridge, April.
- Mufti, A.A. (2002), "Structural health monitoring of innovative Canadian civil engineering structures", *Struct. Health Monit.*, **1**(1), 89-103.
- Mays, G.C. and Tilly, G.P. (1982), "Long endurance fatigue performance of bonded structural joints", *Int. J. Adhes. Adhes.*, **2**(2), 109-113.
- Moyo, P. and Brownjohn, J.M.W. (2002), "Detection of anomalous structural behavior using wavelet analysis", *Mech. Syst. Signal Pr.*, **16**(2-3), 429-445.
- Nowak, A.S. (1993), "Live load model for highway bridges", *Struct. Saf.*, **13**, 53-66.
- Omenzetter, P., Brownjohn, J.M.W. and Moyo, P. (2004), "Identification of unusual events in multi-channel bridge monitoring data", *Mech. Syst. Signal Pr.*, **18**(2), 409-430.
- Pines, D. and Aktan A.E. (2002), "Status of structural health monitoring of long span bridges in the United States", *Struct. Eng. Mater.*, **4**(4), 372-380.
- Ren, Y.M. (2007), *Rain-wind-induced dynamic response analysis of transmission tower-line system*, Master thesis: Dalian University of Technology.
- Schmidt, S. and Solari, G. (2003), "3-D wind-induced effects on bridges during balanced cantilever erection stages", *Wind Struct.*, **6**(1), 1-22.
- The People's Republic of China Ministry of Communications ministerial standard (2004), *General code for design of highway bridges and culverts (JTG D60-2004)*, People Transportation Press, Beijing.
- Wang, M.L. (2004), *State-of-the-art applications in health monitoring*. In: *Invited presentation to workshop on basics of structural health monitoring and optical sensing technologies in civil engineering*, Taiwan: National Central University; 113-42.
- Wu, Z.S. (2003), *Structural health monitoring and intelligent infrastructures in Japan*, (Eds. Wu, Z.S. and Abe,

- M.), Structural health monitoring and intelligent infrastructure. Lisse: Balkema; 153-67.
- Xie, S.M., Jiang, D. and Zhao, W.D. (2000), "An advanced analysis technique sub-modeling and side-frame example", *J. Dalian Railway Institute*.
- Zhang, W., Shi, B., Zhang, Y.F., Liu, J. and Zhu, Y.Q. (2007), "The strain field method for structural damage identification using Brillouin optical fiber sensing", *Smart Mater. Struct.*, **16**(3), 843-850.

CC